2015 American Control Conference
Palmer House Hilton
July 1-3, 2015. Chicago, IL, USA

Plant Modeling for Observer-Based Control of the Link Stabilizing Units at the European X-ray Free-Electron Laser

Michael Heuer, Gerwald Lichtenberg, Sven Pfeiffer, Holger Schlarb and Herbert Werner

***Abstract*— The European X-ray Free-Electron Laser will generate ultra short laser light pulses in the femto-second range to perform experiments with atomic scale resolution. A clock signal synchronizes all components and is distributed by a laser pulses train. These pulses are carried by an optical fiber which is spread through the facility and exposed to external disturbances which change the optical length of the fiber. It is of dire importance to keep this length stable because a change directly results in a timing error of the attached device. For this purpose Link Stabilizing Units are used. This paper shows the modeling of this unit, analyzes their main properties and points out the main control challenges.**

I. INTRODUCTION

A new linear accelerator, called European X-ray Free-Electron Laser (XFEL), is currently under construction at the Deutsches Elektronen Synchrotron (DESY) in Hamburg, Germany. This device with a length of $3.5\,\mathrm{km}$ will generate extremely intense and short X-ray laser light pulses with a duration of a few femto-seconds. To generate these light pulses, electron bunches are accelerated and forced on a sinusoidal trajectory by a periodic arrangement of magnets, called undulator. Further technical specifications of the facility can be found in [1]. These intense and ultra-short X-ray laser pulses provide scientists from all over the world the unprecedented possibility to take a closer look into tiny structures on an atomic scale, [2].

Usually, a synchronization signal is distributed electrically via a coaxial cable. This signal needs to be frequently amplified for long distances in kilometer-range, due to the damping of the cable. This adds noise of the amplifier to the timing signal, which is not suitable for the high timing precision of less than $10\,\mathrm{fs}$ needed for the European XFEL. For that reason, a laser-based synchronization system as proposed in [3] will be used for this facility, [4].

One part of this system is the so-called Link Stabilizing Unit (LSU) which is used to keep the optical length of the fiber constant. This fiber leads the timing signal, an optical pulse train. The main challenge of the LSU is that the controlled value, the timing error of the pulse at the end-station, is not measured directly. Just the error of a returning pulse at the start of the LSU is measurable. Moreover, this measurement is time delayed with respect to the actuator and the controlled value. For that reason, a model of the system has to be found in order to build the observer-based control structure shown in Fig. 1. This will be explained in in section IV. Additionally, it is verified whether the position of the actuators and sensors are feasible for the control purpose.

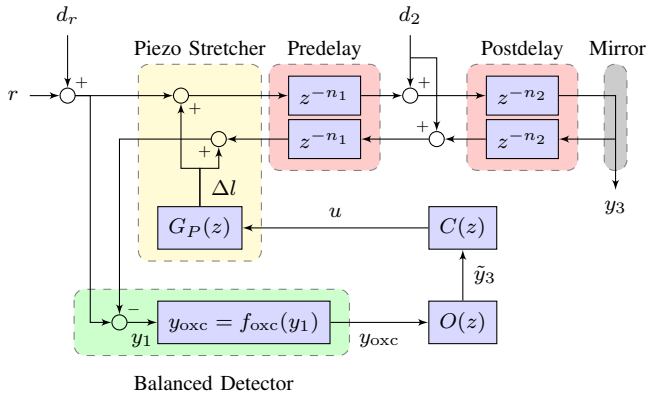

Fig. 1. Block Diagram of the LSU in the current experimental setup, including the actuator, the Piezo Stretcher, the measurement device, the Balanced Detector, and the fiber modeled with delay elements. The observer $O(z)$ and the controller $C(z)$ should stabilize the output y_3.

This paper is organized as follows: Section II gives an overview of the laser based synchronization system and shows how to model the pulse train. The next section explains how to model the Fiber Link of the Link Stabilizing Units in a general case. In Section IV, the actuator and sensor parameter of the current setup are introduced, followed by the analysis and identification of the experimental laboratory setup, given in Section V. The paper closes with a short outlook how to improve the model and with first ideas on control.

II. LASER BASED SYNCHRONIZATION SYSTEM

Figure 2 shows a simplified version of the laser based synchronization system and the beamline of the accelerator. The injector laser triggers a detachment of electrons at the cathode of the gun. The generated cloud of electrons, the so called electron bunch, is accelerated by 101 superconducting modules (I0 and I39H, A1.M1-4, ..., A25.M1-4). An explanation of this modules is given in [5]. At the end of the beamline, the electron bunch is lead through the undulator which forces the electrons on a sinusoidal trajectory and generates ultra short X-ray flashes.

M. Heuer, S. Pfeiffer and H. Schlarb are with the Deutsches Elektronen Synchrotron Notkestraße 85, 22607 Hamburg, Germany {michael.heuer, sven.pfeiffer, holger.schlarb}@desy.de

G. Lichtenberg is with the Hamburg University of Applied Sciences, Ulmenliet 20, 21033 Hamburg, Germany gerwald.lichtenberg@haw-hamburg.de

H. Werner is with the Hamburg University of Technology, Schwarzenberstrae 95, 21073 Hamburg, Germany h.werner@tu-harburg.de

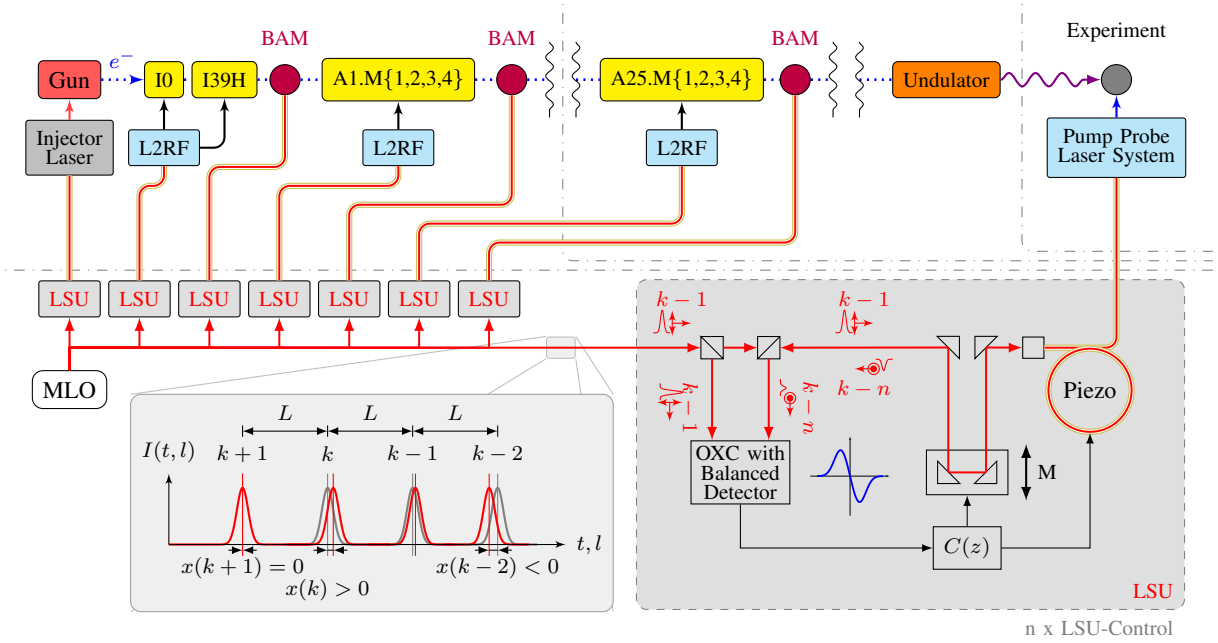

Fig. 2. Overview of the European XFEL beamline and the connected laser-based synchronization system. The Master Laser Oscillator (MLO) generates an equidistant laser pulse train and the Link Stabilizing Units (LSU) keeps the optical length of the attached fiber constant to a multiple of the period length L of the laser pulse train.

To provide a clock signal to the devices, a laser-based synchronization system is used. It consists of two parts, the Master Laser Oscillator (MLO) generates the laser pulse train, i. e., the timing signal of the system, which is distributed through fibers to the different end stations in the facility. How to model the MLO is given in [6]. The graph in the lower left part of Fig. 2 shows the pulse intensity $I(t, l)$ of the pulse with respect to time t and position in the fiber l of the pulse train. The distance between two pulses L is given by the repetition rate of the MLO.

The fiber is exposed to temperature and humidity changes as well as vibrations, which results in small changes of its optical length. To stabilize this length, the second part of this system, the LSU is used. If a pulse enters the LSU, a small fraction of the laser pulse is branched off and the main part goes through a piezo stretcher and into the fiber to the device in the accelerator. The piezo stretcher allows to slightly change the length of the fiber. To compensate bigger changes, which exceed the piezo range, a coarse tuning Motor (M) is used. At the device, the pulse is partially reflected and travels back the way to the LSU. This returning pulse and the fraction of the subsequent pulse are guided through an Optical Cross Correlator (OXC). This nonlinear crystal generates a correlation of the two pulses and is passed twice. With the two correlations, a balanced detector can detect the timing difference between both incoming pulses. If the output of the balanced detector is zero, the length of the attached fiber is a multiple of the MLO repetition rate. With this scheme it is possible to suppress the error of the timing signal caused by length changes of the fiber. The performance of LSU depends on a stable laser pulse train.

III. STRUCTURE OF THE OPTICAL FIBER WITH REFLECTOR

In this section, the fiber with the reflection at the end is discussed, in combination with the basic measurement principle of time differences. Furthermore the choice of positioning the actuator and sensor is investigated.

A. Functional block diagram

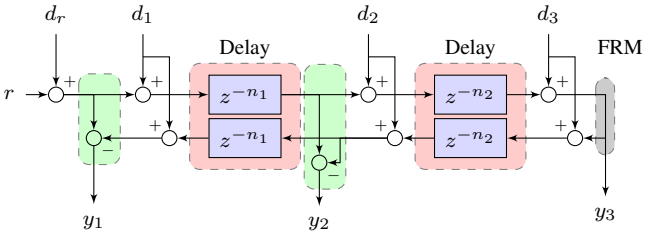

Fig. 3. Block Diagram of the optical fiber with a mirror at the end, including the reference input r, different disturbance inputs d_* and measurement positions y_*.

Figure 3 shows the fiber link in a general simplified case. The signal d_r represents the timing error of the incoming pulse train. The reference value r can be used to achieve a constant shift of the pulse train and the disturbance inputs $d_{1,2,3}$ are small length changes – compared to the period length of the pulse train – at different positions of the fiber. If an actuator, such as a piezo stretcher, is attached at a point of the fiber, the length change due to that piezo acts exactly as a disturbance. Therefore the disturbances $d_{1,2,3}$ lead to

the same effects as an input (later Δl) if a piezo actuator is considered at this point. The disturbance d_1 is active at the beginning and d_3 at the end of the fiber. Choosing the delays $n_1, n_2 \in \mathbb{N}_0^+$, d_2 can model a disturbance at an arbitrary point of the fiber. At the end of the fiber link, a Faraday Rotating Mirror (FRM) transmits a part of the pulse y_3 and reflects another part, going back through the fiber. The output y_3 should be stabilized, but it is not measurable in the final setup. In addition, available measurement device at, e. g., $y_{1,2}$ are only capable of measuring the relative error between two pulses. Based on the structure in Fig. 3, this can be modeled as a discrete state space model:

$$x(k+1) = \Phi x(k) + \Gamma d(k)\,, \tag{1}$$

$$y(k) = Cx(k) + Dd(k)\,, \quad \text{with} \tag{2}$$

$$y(k) = \begin{pmatrix} y_3(k) \\ y_2(k) \\ y_1(k) \end{pmatrix}, \quad d(k) = \begin{pmatrix} d_r(k) \\ d_1(k) \\ d_2(k) \\ d_3(k) \end{pmatrix}, \quad n = n_1 + n_2\,, \tag{3}$$

$$\Phi = \left[\begin{array}{ccc:c} 0 & \dots & 0 & 0 \\ \hdashline & & & 0 \\ & I^{2n-1\,\times\,2n-1} & & \vdots \\ & & & 0 \end{array}\right], \tag{4}$$

$$\Gamma = \begin{bmatrix} 1 & 1 & 0^{n_1\,\times\,1} & 0^{n\,\times\,1} \\ 0^{2n-1\,\times\,2} & & 1 & \vdots \\ \vdots & \vdots & 0^{2n_2-1\,\times\,1} & 2 \\ \vdots & \vdots & 1 & 0^{n-1\,\times\,1} \\ \vdots & \vdots & 0^{2n_2-1\,\times\,1} & \vdots \end{bmatrix}, \tag{5}$$

$$C = \begin{bmatrix} 0^{1\,\times\,n-1} & \dots & 1 & 0^{1\,\times\,n} & \dots \\ 0^{1\,\times\,n_1+2n_2-1} & \dots & -1 & 0^{1\,\times\,n_1} & \dots \\ 0^{1\,\times\,2n} & \dots & \dots & \dots & -1 \end{bmatrix}, \tag{6}$$

$$D = \begin{pmatrix} 0 & 0 & 0 & 1 \\ 0 & 0 & -1 & 0 \\ 1 & -1 & 0 & 0 \end{pmatrix}. \tag{7}$$

With the model given in (1 - 7), the following sections analyze basic system properties in order to verify the choice of the actuator and sensor position.

B. Controllability and Observability

Controllability and Observability are two fundamental properties of state space models, which describes whether it is possible to drive all states $x(k)$ with the available control input $u(k)$ to a certain value and if it is possible to recover all states $x(k)$ from the given measurements $y(k)$, [7]. It is important to choose the actuator and the sensor in a way that both properties are fulfilled.

The system is controllable if and only if the controllability matrix

$$\mathcal{C} = \begin{bmatrix} \Gamma_{d_i} & \Phi\Gamma_{d_i} & \Phi^2\Gamma_{d_i} & \cdots & \Phi^{n-1}\Gamma_{d_i} \end{bmatrix} \tag{8}$$

has full rank.

In the final setup, just one actuator should be used, therefore only single inputs are considered. For that case, just the sub-matrix of Γ called Γ_{d_i}, corresponding to the input d_i , $i = r, 1, 2, 3$, is used. Since $\mathcal{C}_{d_r}$ and $\mathcal{C}_{d_1}$ are identity, the system is controllable via each of the inputs d_r and d_1. For the single inputs d_2 and d_3 the rank condition is not fulfilled. The system is observable if and only if the observability matrix

$$\mathcal{O} = \begin{bmatrix} C_{y_i}^T & (C_{y_i}\Phi)^T & (C_{y_i}\Phi^2)^T & \cdots & (C_{y_i}\Phi^{n-1})^T \end{bmatrix}^T \tag{9}$$

has full rank. As in the controllability case, only single outputs y_i, with $i = 1, 2, 3$ and the corresponding output matrix C_{y_i}, are considered. The system is only found to be observable from the output port y_1. For both other channels the observability condition is not fulfilled.

This section shows that the intuitive way, to put the actuator and the sensor at the beginning of the fiber link, is the right choice and this planned configuration can be used to control this plant.

C. Transmission zeros

The structure with the delayed relative measurement leads to transmission zeros which could decreases the control performance. In order to determine, for which frequencies a reference change r or a disturbance d_r are not visible at the output y_1, it is possible to transform the discrete time system into a continuous one using $z = e^{sT}$ and studying the frequency response with $s = j\omega$. This leads to the transfer function

$$G_{y_1 d_r}(j\omega) = 1 - e^{j\omega T(-2n_1-2n_2)}\,. \tag{10}$$

For a given fixed fiber length $n = n_1 + n_2 = \text{const.}$, pulse length T and frequencies of

$$\omega_{dr,n,a} = \frac{\pi a}{Tn}\,, \quad a \in \mathbb{N}_0^+ \tag{11}$$

the magnitude of the transfer function in (10) goes to zero. This means that disturbances with such frequencies are not transmitted to the output.

The same effect also applies for disturbances acting on the fiber in the accelerator tunnel. Using the same method as before the frequency response for $\omega = 2\pi f$ at an arbitrary position defined by n_1 and n_2 gives

$$G_{y_1 d_2}(j\omega) = \left(-1 - e^{j\omega 2Tn_2)}\right) e^{-j\omega Tn_1}\,. \tag{12}$$

A disturbance d_2 with frequencies of

$$\omega_{d_2,n_2,a} = \frac{2\pi a + \pi}{-2Tn_2}\,, \quad a \in \mathbb{N}_0^+ \tag{13}$$

would not be transmitted to the output y_1.

This section shows that some disturbances on the reference input as well as some acting on the fiber in the tunnel are not visible at the measurement device but on the output which is to be controlled. This limits the maximum performance of the system.

IV. ACTUATOR AND SENSOR FOR THE LSU

After examination of the fiber link properties, the next section discusses the properties of the actuator and sensor. Recall Fig. 1 showing the block diagram of the LSU setup, including the planned observer and controller.

A. Piezo Stretcher

To adjust the length of the fiber, a piezo stretcher is used which causes small timing changes. The change Δl is induced due to the length change of the fiber which is wrapped around a disk shaped piezo crystal. This change has the same effect as the disturbance d_1 and $d_1 = \Delta l$ can be used to connect the piezo model to the fiber model. As a first attempt, the transfer function of the piezo stretcher, which maps the applied voltage u to a length change Δl, is modeled as a second order system

$$G_p(z) = \frac{\Delta l(z)}{u(z)} = \frac{b_0 + b_1 z^{-1} + b_2 z^{-2}}{1 + a_1 z^{-1} + a_2 z^{-2}}\,. \tag{14}$$

This of course neglects higher order modes of the crystal and nonlinear effects like hysteresis or creep. Those latter were not observed in previous experiments and thus are neglected in this first approach.

B. Balanced Detector

To measure the timing error between two $n \in \mathbb{N}^+$ sample separated pulses, an OXC in combination with a balanced detector is used as described in the introduction. A main characteristic of that device is the much lower bandwidth compared to the pulse frequency. Hence a continuous time signal, which represents the average of the timing error of an arriving pulse, can be measured. The nonlinear function describing the output voltage of the device is given by

$$y_{\text{oxc}}(k) = f_{\text{oxc}}(y_1(k)) =$$

$$\frac{P_+}{\cosh^2\left(\frac{d_+ + y_1(k)}{a_+}\right)} - \frac{P_-}{\cosh^2\left(\frac{d_- - y_1(k)}{a_-}\right)} + b\,, \tag{15}$$

where the power of the correlation pulses are $P_\pm$, the pulse duration is given by $a_\pm$. The shift of the center $d_\pm$ is dependent on mechanical setup of the LSU and b represents the bias voltage of the balanced detector. This function is shown in Fig. 4.

The linear region, shown as a dashed line close to the y axis of the graph, can be used for a linear approximation.

V. LSU AT THE EUROPEAN XFEL

In this section, the characteristics for the LSUs at the XFEL are evaluated using the equations derived before. A laboratory test setup is used to identify the nonlinear function of the balanced detector and the transfer function of the piezo stretcher.

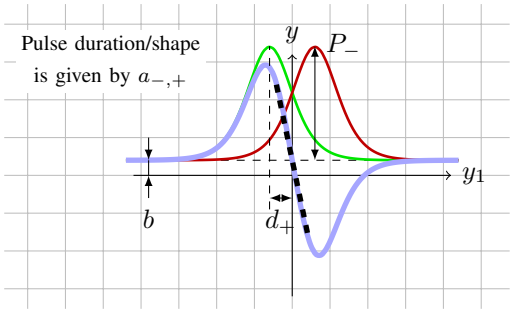

Fig. 4. Nonlinear mapping function of OXC (——) , with the linear region (▪ ▪ ▪), the positive (——) and negative (——) correlation of the two measured pulses.

A. System parameters

The repetition rate of the generated laser pulse train is

$$T = \frac{1}{f} = \frac{1}{216.66\,\text{MHz}},$$

therefore, two consecutive pulses (k and $k+1$) are separated by the period time of $4.615\,\text{ns}$. The period length (in a fiber with a refraction index of $n_R = 1.4$) is

$$L = \frac{v}{f} = \frac{c}{n_R f} = \frac{3 \cdot 10^8\,\frac{\text{m}}{\text{s}}}{1.4 \cdot 216.66\,\text{MHz}} = 0.989\,\text{m}\,.$$

The time delays n_1, n_2 and $n = n_1 + n_2$ are determined by the overall length of the fiber l, which consists, in the longest case, of the single mode fiber in the tunnel itself ($\approx 3600\,\text{m}$), a dispersion compensating fiber ($\approx 480\,\text{m}$) and the fiber around the piezo crystal ($\approx 22\,\text{m}$). This leads to a one way delay of

$$n = n_1 + n_2 = \frac{l}{L} = \frac{4102\,\text{m}}{0.989\,\text{m}} \approx 4154\,\text{samples}$$

and a total delay of $2n$ from the reference r to the output y_1. Hence a disturbed pulse will travel $4154\,\text{samples}$ ($19.17\,\mu\text{s}$) to the output y_3. After that, it will again travel this amount of samples before the timing error will be determine with another disturbed pulse arriving at the LSU from the MLO $8308\,\text{samples}$ after that one.

B. Influences of reference disturbances

To determine which frequencies are not visible at the measurement output y_1, generated by the MLO on the input d_r, equation (11) is used. This leads to frequencies of

$$\omega_{d_r,2,a} \approx a \cdot 68 \cdot 10^6\,\frac{\text{rad}}{\text{s}} \approx a \cdot 10.8\,\text{MHz} \tag{16}$$

for a $0.989\,\text{m}$ long link down to

$$\omega_{d_r,8304,a} \approx a \cdot 16.4 \cdot 10^3\,\frac{\text{rad}}{\text{s}} \approx a \cdot 2.6\,\text{kHz} \tag{17}$$

for a $4108.30\,\text{m}$ long link.

Figure 5 shows the magnitude of the transfer function from the disturbance d_r to the measurement output y_1. For low frequencies and a constant offset of the disturbance d_r, the magnitude goes to zero. This means that a steady state error

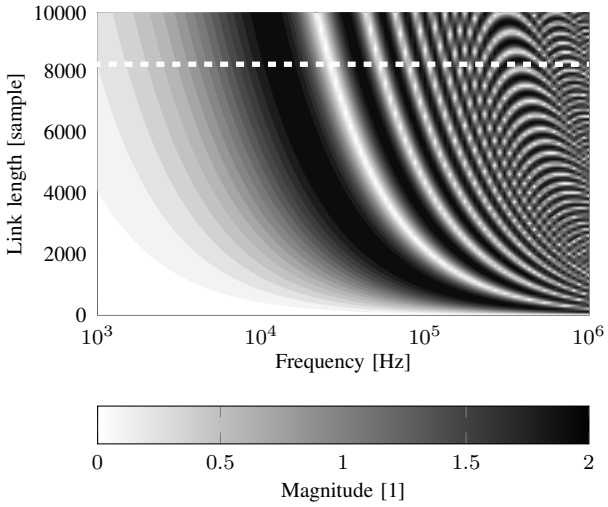

Fig. 5. Magnitude of $G_{y_1 d_r}(z)$ for different fiber lengths.

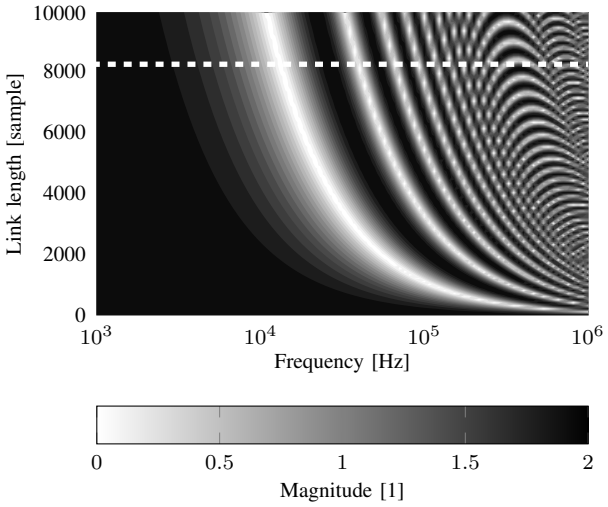

Fig. 6. Magnitude of $G_{y_1 d_2}(z)$ dependent on the distances to the link end.

of the pulse train is not visible for the link measurement output y_1 but is transmitted to the output y_3. Therefore reaching a zero steady state error for y_3 depends on the mean value of d_r and the steady state value of the MLO system.

Another effect of this behavior could result in a wrong rating of the link performance. Right know the performance of a link is measured by the root mean square of the measured output y_1. If a reference disturbance d_r, is in a range where its double magnitude is measured, user may assume that the performance of one link is worse than an other link where the disturbance is not measurable due to the link length, even if the second link has a better performance on the output y_3 which is of interest.

A possible solution is to use the error signal of the MLO for a disturbance feedforward control or combining the measurement of multiple links with different lengths. This could also allow a separation of different disturbance sources.

C. Influences of disturbances acting on the fiber

With (13) and a disturbance d_2 at a position defined by n_2, not measurable frequencies on y_1 are

$$\begin{aligned}\omega_{d,2,a} &\approx a \cdot 68 \cdot 10^6 \,\frac{\text{rad}}{\text{s}} + 34 \cdot 10^6 \,\frac{\text{rad}}{\text{s}} \\ &\approx a \cdot 10.8\,\text{MHz} + 5.9\,\text{MHz}\end{aligned} \tag{18}$$

close to the end station ($n_2 = 1$) and

$$\begin{aligned}\omega_{d,8304,a} &\approx a \cdot 16.4 \cdot 10^3 \,\frac{\text{rad}}{\text{s}} + 8.2 \cdot 10^3 \,\frac{\text{rad}}{\text{s}} \\ &\approx a \cdot 2.6\,\text{kHz} + 1.3\,\text{kHz}\end{aligned} \tag{19}$$

far away from the end station ($2n_2 = 8304$).

Figure 6 shows the magnitude of the transfer function from the disturbance d_2 to y_1 for different positions of the fiber and the effect on y_1 of an input to the piezo which produces a length change Δl. Contrary to the reference disturbance, in this case a constant offset is measurable, but with the double amplitude. A problem due to the zeros in this transfer function is that disturbances, e. g., induced by the characteristic frequency of the piezo stretcher and the harmonics of a higher order are not visible to the measurement device but present at the real output y_3.

D. Identification of Balanced Detector

To identify the characteristics of the balanced detector a slow voltage sweep on u is performed and shown in Fig. 7.

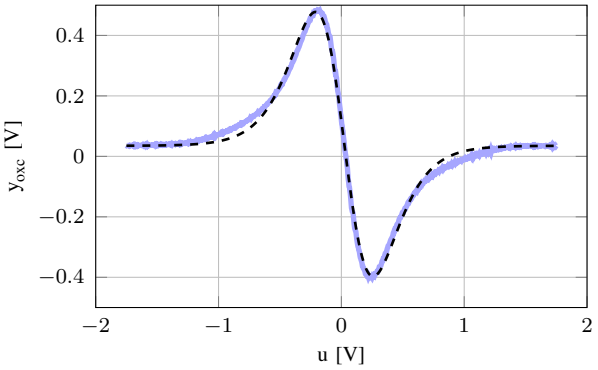

Fig. 7. Measurement ( ) and identification ( ) of the optical cross correlator

The linear range of this configuration covers an input u of $[-0.1, \ldots, 0.1]\,\text{V}$ which generates an output y_{oxc} of $[-0.42, \ldots, 0.38]\,\text{V}$. For the identification and in later applications, the balanced detector should be operated in this range.

E. Identification of the piezo stretcher transfer function

In this section, the transfer function $G_{yu}(z)$ which maps the applied voltage u to the output y, is identified in an open-loop manner. One challenge during this procedure is to stay in the linear range of the balanced detector during the excitation as described before.

The measurement is performed on a Micro Telecommunications Computing Architecture enhancements for rear I/O and precision timing (MicroTCA.4) system which offers an ADC with an input range of $[-1, 1]\,\mathrm{V}$ with $16\,\mathrm{bit}$ at $125\,\mathrm{MHz}$, a DAC with an output range of $[-1, 1]\,\mathrm{V}$ with $16\,\mathrm{bit}$ at $250\,\mathrm{MHz}$ and a Virtex 6 FPGA which performs the required computation tasks. In this setup, all components are driven with $81\,\mathrm{MHz}$. Due to the limited storage capacity, the data acquisition is downsampled by a factor of 256, which leads to a sampling rate of the discrete time system of $316.4\,\mathrm{kHz}$, a sample time of $3.16\,\mu\mathrm{s}$ and a rate change compared to the $216.66\,\mathrm{MHz}$ system of 685.

The available link in the laboratory setup has a length of $320\,\mathrm{m}$ and therefore the delay in samples of the pulse train is given by $n = 647$. The delay due to this length of the fiber is lower than the sampling rate and the first occurring zero is also neglectable. For that reasons it is assumed that

$$G_{yu}(z) = 2 \cdot G_P(z)\,. \tag{20}$$

For this downsampled setup and a $3.5\,\mathrm{km}$ long link with the maximum $8308\,\mathrm{samples}$ w.r.t. to the pulse train, the time delay of z^{-2n} compared to the controller sampling rate would be $12\,\mathrm{sample}$ and is not negligible.

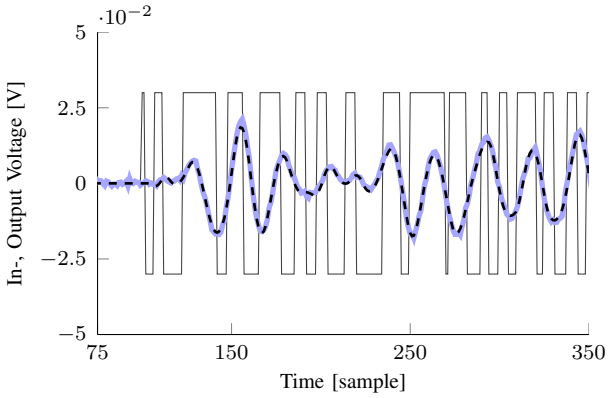

Fig. 8. Cross-validation of $G_{yu}(z)$ (- - -) against a measurement (——) generated by a prb input signal (——). The fiber link has a length of $300\,\mathrm{m}$ and the data are downsampled by a factor of 256

Figure 8 shows the cross-validation of the transfer function

$$G_{yu}(z) = \frac{-0.008549 z^{-1}}{1 - 1.942 z^{-1} + 0.9955 z^{-2}} \tag{21}$$

which is identified using a PRB signal as an excitation. The characteristic frequency of the piezo crystal is

$$f_{0,P} \approx 18.5\,\mathrm{kHz}\,.$$

Based on the data sheet of the piezo, the guess for the first harmonic is assumed to be $18\,\mathrm{kHz}$. The signal for the identification was therefore chosen in such a way, that it covers a wide frequency range around this frequency.

As given in Section IV-A, the transfer function for the piezo stretcher $G_P(z) = 0.5 \cdot G_{yu}(z)$ can be expressed using (14). If the system given by (1 - 7) is scaled to the appropriate sampling time, both system can be connected using the method shown in Section IV-A. The output y_1 of this model can then be mapped with the nonlinear behavior of the Optical Cross Corrrelator (OXC) which gives the whole nonlinear system model.

VI. CONCLUSIONS AND FUTURE WORK

This paper shows how to model the Link Stabilizing Units used at the new European XFEL. The important system properties and challenges are outlined, e. g., that the output to be stabilized and the measured output are different. Therefore, an observer-based structure has to be used. It is shown that the longest link has a time delay which influences the dynamic behavior of the system and should not be neglected.

To cope with this property, it is planed to include a smith predictor scheme. If the limited operation range of the setup, due to the nonlinear sensor function, is too restrictive, the problem could be addressed with an extended Kalman Filter. This kind of filter is, e. g., explained in [8].

From the modeling point of view, it is possible to include the measurement of the piezo current to the model. This additional information is expected to yield to better results. Since with such a measurement, it should be possible to include a hysteresis model for the piezo, which approximates the real behavior closer.

In order to design and synthesize a controller to stabilize the output of that plant, different classical controller types, as a LQG controller with a smith predictor will be evaluated. The advantage of the new control system, based on the MicroTCA.4 architecture and FPGAs for the computation of the control algorithm, is that complex control strategies can be implemented.

REFERENCES

[1] M. Altarelli, R. Brinkmann, M. Chergui, W. Decking, B. Dobson, S. Düsterer, G. Grbel, W. Graeff, H. Graafsma, J. Hajdu, J. Marangos, J. Pflüger, H. Redlin, D. Riley, I. Robinson, J. Rossbach, A. Schwarz, K. Tiedtke, T. Tschentscher, I. Vartaniants, H. Wabnitz, H. Weise, R. Wichmann, K. Witte, A. Wolf, M. Wulff and M. Yurkov, The European X-Ray Free-Electron Laser Technical design report, Deutsches Elektronen-Synchrotron, Hamburg, Germany, 2007.

[2] C. M. Günther, B. Pfau, R. Mitzner, B. Siemer, S. Roling, H. Zacharias, O. Kutz, I. Rudolph, D. Schondelmaier, R. Treusch and S. Eisebitt, Sequential femtosecond X-ray imaging, Nature Photonics 5, 2011, pp. 99-102.

[3] J. W. Kim, F. Ö. Ilday, F. X. Kärtner, O. D. Mücke, M. H Perrott, W. S. Graves, D. E. Moncton and T. Zwart, Large scale timing distribution and RF-synchronization for FEL facilities, Proc. Free Electron Laser Conference 2004, Trieste, Italy, 2004.

[4] S. Schulz, M. Bousonville, M. K. Czwalinna, M. Felber, M. Heuer, T. Lamb, J. Müller, P. Peier, S. Ruzin, H. Schlarb, B. Steffen, F. Zummack, T. Kozak, P. Predki and A. Kuhl., Past, Present and Future aspects of Laser-Based Synchronization at FLASH, Proc. International Beam Instrumentation Conference 2013, Oxford, U.K., 2013.

[5] S. Pfeiffer, G. Lichtenberg, C. Schmidt, H. Schlarb, H. Werner, Design of an Optimal and Robust Controller for a Free-Electron Laser Exploiting Symmetries of the RF-System, Proc. 51st IEEE Conf. Decis. Control., Maui, Hawaii, USA, 2012, pp. 42534258.

[6] M. Heuer, G. Lichtenberg, S. Pfeiffer, H. Schlarb, C. Schmidt and H. Werner, Modeling of the Master Laser Oscillator Phase Noise for the European XFEL using Fractional Order Systems, Proc. 19th IFAC World Congress, Cape Town, South Africa, 2014.

[7] S. Skogestad and I. Postlethwaite, Multivariable Feedback Control: Analysis and Design, Wiley, Chichester, U.K., 2001.

[8] M. S. Grewal and A. P. Andrews, Kalman Filtering: Theory and Practice Using MATLAB, Wiley, Chichester, U.K., 2001.